J Nanostruct 13(1): 122-131, Winter 2023

RESEARCH PAPER

The Effects of Solvent Treated PEDOT:PSS Layer to Enhance Polymer Solar Cells Efficiency

Mohammed K. Al Hashimi [1], Buraq T. SH. AL-Mosawi [1], Burak Yahya Kadem [2]*

[1] *Department of Physics, College of Education, University of Misan, Maysan, Iraq*

[2] *College of Science, Al-Karkh University of Science, Baghdad, Iraq*

ARTICLE INFO

Article History:
Received 05 October 2022
Accepted 26 December 2022
Published 01 January 2023

Keywords:
Organic solar cells
PCPDTBT:PC61BM
PCPDTBT: PC71BM: SWCNTs
PEDOT:PSS
Solvent treatment

ABSTRACT

The present work is a detailed study of the poly(3,4-ethylenedioxyt hiophene):poly(styrenesulfonate) PEDOT:PSS films, were made to undergo different treatments to examine how they affected morphology, conductivity, transmittance, as well as the relative effect of the way the organic photovoltaic devices performed. This was done by using the PCPDTBT:PC_{71}BM:SWCNTs and PCPDTBT:PC_{61}BM mixtures. The process involves using DMSO and EG solvents for doping PEDOT:PSS and separately exposing the films to the vapour of ammonium hydroxide (NH4OH) solvent. After doping solvent was added to the PEDOT:PSS solution, , the conductivity and transmittance of PEDOT:PSS experienced a substantial increment, after which solvent treatment was performed by subjecting these films to NH4OH solvent. When devices were doped using PCPDTBT:PC_{71}BM:SWCNTs or PCPDTBT:PC_{61}BM with power conversion efficiency, The optimal organic photovoltaic devices achieved a 3.68% as compared to 2.20% for pristine PV devices or 2.67% instead of 1.51% for pristine devices, respectively. The solvent treatment played a significant part in enhancing conductivity in PEDOT:PSS films.

How to cite this article
Al Hashimi M K., AL-Mosawi B T., Kadem B Y. The Effects of Solvent Treated PEDOT:PSS Layer to Enhance Polymer Solar Cells Efficiency. J Nanostruct, 2023; 13(1):122-131. DOI: 10.22052/JNS.2023.01.014

INTRODUCTION

In molecular electronic devices, there is a high use of poly (ethylene-3,4-dioxythiophene): poly (styrene sulfonic acid) (PEDOT:PSS) in the form of a transparent anode that has a comparatively high work function. In addition, it is also used as a smoothing layer to coat the coarse inorganic conducting surfaces (typically indium-tin oxides [1]. It is widely acknowledged as a highly appropriate conductive polymer that are employed as a hole-transporting layer as it has high transparency, easy processing, and stability. There is extensive use of PEDOT:PSS as an anode interfacial layer that improves the anode contact and also increases the hole transmitting the polymer solar cells [2]. There is a substantial increase in the electrical conductivity of PEDOT:PSS with the inclusion of a few organic solvents [3,4], and acids [5], to the PEDOT:PSS. However, there continues to be a lack of clarity on how this increase is brought about. The findings from the literature also show that two contradictory effects are caused by the annealing process on film conductivity, which is typically used as a critical step when formulating the device. These are modifications in the surface ratio of PEDOT:PSS [3,4,6] and the screening impact of the solvent [7]. In comparison to the films created from pristine aqueous solutions, the

* *Corresponding Author Email: mr.mohammed@uomisan.edu.iq*

technique used for the production of the film from the mixture in which there is aqueous distribution of the polymer and an organic additive often gives rise to more rough film morphology [7]. There is widespread acknowledgment of PEDOT:PSS being a combination of conjugated conducting polymer PEDOT and non-conjugated water-soluble PSS polymer [8]. It has been determined that there is an increase in the charge carrier concentration in 5 wt.% dimethyl sulfoxides (DMSO) doped PEDOT:PSS films when sodium hydroxide (NaOH) is used to regulate the pH level of the polymer [9]. The findings of various studies have shown that the conductivity of PEDOT:PSS increases substantially when aqueous PEDOT:PSS solution is treated using different solvents, e.g., ethanol, methanol, glycerol, isopropanol, ethylene glycol, D-sorbitol, and diethylene glycol. This increase was because of the removal of the PSS component in the PEDOT:PSS films to a certain degree [10-12]. In organic solar cells (OSC) devices, Vosgueritchian et al. [13] have employed the most conductive preparation of PEDOT:PSS (CLEVIOS PH 1000).. According to the authors, when fluorosurfactant was included as an additive in PEDOT:PSS, there was a 36% increase in sheer resistance (Rs) in comparison to PEDOT:PSS thin films that were not treated. In addition, EG/PH1000 PEDOT:PSS doped with graphene are made to undergo spray coating to create large area and extremely conductive films with exceptional mechanical properties which are employed as ultrathin electrode in organic solar cells (OSC) devices [14]. Au nanoparticles are used to dope PEDOT-PSS AI4083, which is another kind another kind of PEDOT:PSS conductive ink that is also employed in OSC devices [15]. When Au nanoparticles are increased in PEDOT:PSS, efficiency increases by around 13% to become 3.51%. This increase occurs because of the increase in FF from 0.58 to 0.62 and in J_{sc}, from 8.7 mA/cm^2 to 8.94 mA/cm^2. When the ratio of Au nanoparticles increases further, device performance is affected negatively [16]. The use of spin coating methods makes it possible for PEDOT:PSS to create a transparent film with low sheet resistance and high conductivity [17]. For different uses of PEDOT:PSS thin films, it is important to combine conductivity and morphology [1]. While the drying process is being carried out, there are various factors that could affect these films, such as the proportion of solid content, PSS percentage, particle size, and the solution viscosity, because of which distinct morphological and electrical properties are developed [18]. In addition, the power conversion efficiency (PCE) fundamentally determines the solar performance, and this is dependent on various parameters, e.g., exciton production, the active layer's light harvesting, diffusion, separation, transportation, and collection by the electrode [19]. The production of organic solar cells (OSCs) devices from the combination of (PCDTBT: $PC_{71}BM$) bulk heterojunction systems exhibit comparatively improved photovoltaic (PV) properties in comparison to the rest of bulk heterojunction organic solar cells (OSCs) [20]. This study has examined the impact of PEDOT:PSS treated with Ethylene glycol (EG) and Dimethyl Sulfoxide (DMSO). PEDOT:PSS is typically treated with solvent additives or with solvent vapour treatment. Two techniques were used in this study. In the first, PEDOT:PSS is doped with DMSO or EG. The other technique is using a solvent to treat the doped PEDOT:PSS layer (utilizing the performing NH4OH solvents treatment for DMSO -doped PEDOT:PSS layer). There is a direct effect of this treatment on the morphology, optical, electrical conductivity, and other properties of the PEDOT:PSS layer, and hence, on the organic solar cells' effectiveness.

MATERIALS AND METHODS

Materials and Chemicals

The following were bought from Sigma Aldrich: Poly (3,4ethylenedioxythiophene): poly (styrene sulfonate) (PEDOT:PSS) layer (PH1000), Ethylene glycol (EG), Ammonium hydroxide (NH4OH), indium doped tin oxide (ITO) (having thickness of 80 nm and sheet resistance of 25 Ω/sq), Dimethyl Sulfoxide (DMSO), chlorobenzene (CB), [6,6]-Pheny C_{61} butyric acid methyl ester ($PC_{61}BM$), (6,6)-Phenyl C_{71} butyric acid methyl ester and Poly[9-(1-octylnonyl)-9H-carbazole-2,7-diyl]-2,5-thiophenediyl-2,1,3-benzothiadiazole-4,7-diyl-2,5-thiophenediyl (PCDTBT), and a mixture of isomers ($PC_{71}BM$).

PEDOT Doping: PSS with EG and DMSO

The hole transport layer (HTL) in the organic cell was created from PEDOT:PSS aqueous solution (PH1000). The PEDOT:PSS layer was altered in two steps. First, 0.6 ml of EG and DMSO were separately inserted into 12 ml PEDOT:PSS in the form of additives [21, 22]. After this, vigorous mixing of the solution was carried out for five hours, following

which it was passed through a 0.45-µm polyvinyl difluoride filter. The spin coating was then carried out at 2000 rpm for 30 seconds to deposit the filtered PEDOT:PSS over the ITO substrates. The thin film thickness is determined using spectroscopic ellipsometry, which is determined to be 100 nm [23], and minor variations are observed between the thin films examined. Water, methanol, and ethanol were used to pre-clean the ITO-coated glass in an ultrasonic bath for 10 minutes each. Doped PEDOT:PSS and pristine were annealed at a temperature of 120° C for 30 minutes. The doped-PEDOT:PSS layer was then made to undergo additional solvent treatment for two hours each. Solvent treatment was also carried out on DMSO-doped PEDOT:PSS layer and the EG-doped PEDOT:PSS. Following the treatment, they were annealed at a temperature of 120° C for 30 minutes.

Sample Preparation

$PC_{71}BM$ and PCDTBT were immersed in chloroform or chlorobenzene in a 1:1 ratio, after which they were mixed at 60° C for 1 hour. To this (PCDTBT: $PC_{71}BM$) solution, SWCNTs were added in volumes (1:1:0:5), which were sonicated for 1 hour. PCDTBT:$PC_{61}BM$ (in 1:1 ratio) were then separately added to in chlorobenzene, and mixed at 70° C overnight to create the organic ink. Spin coating of the active layers was carried out over the PEDOT:PSS layers within a N_2-filled glove box, after which they were annealed within the glove box for 10 minutes at a temperature of 120° C. The TiO_2 layer was developed over the PCDTBT:$PC_{71}BM$:SWCNTs active layer, After that, it was annealed for 10 minutes at 120 ° C on a hot plate within a glove box filled with nitrogen, bringing about the development of 40 nm thick films.

A quartz crystal thickness monitor was used to monitor the evaporation of a top contact of aluminium (Al) that was around 100 nm thick, with a deposition rate ranging between 0.1 and 0.2 nm/sec. Further heat treatment was carried out on all the devices within the glove box at a temperature of 120° C for 10 minutes, after which they were allowed to cool for 30 minutes, following which measurements were obtained. The devices diagram of the PCDTBT: $PC_{71}BM$:SWCNTs and PCPDTBT:$PC_{61}BM$-based devices being investigated is demonstrated in Fig. 1.

Characterization

A Varian Cary 5000 UV-Vis-NIR spectrophotometer that operates between 190 to 1100 nm is used to record the optical properties of the layers being examined. The multipurpose X'Pert Philips X-ray diffractometer (MPD) was used to examine the blend structure (Cu, k = 0.154 nm). A Veeco Nano-Scope IV Multi-Mode AFM in tapping mode was used to identify the films' morphology. A Raman spectrometer (Renishaw, UK) that had an excitation wavelength of 514 nm was used to determine the Raman properties. A 2400 computerized source meter was used to examine the DC electrical properties, which included current-density voltage (J-V) dependence and electrical conductivity of PEDOT:PSS layers and completed OSC devices. Also, With a AM 1.5 solar simulator source of 100mW/cm^2, the photocurrent was generated; for the I-V characterization, a shadow mask was employed that had the same active area (0.07 cm^2). The equations given below [22] were used to compute the solar cell's fill

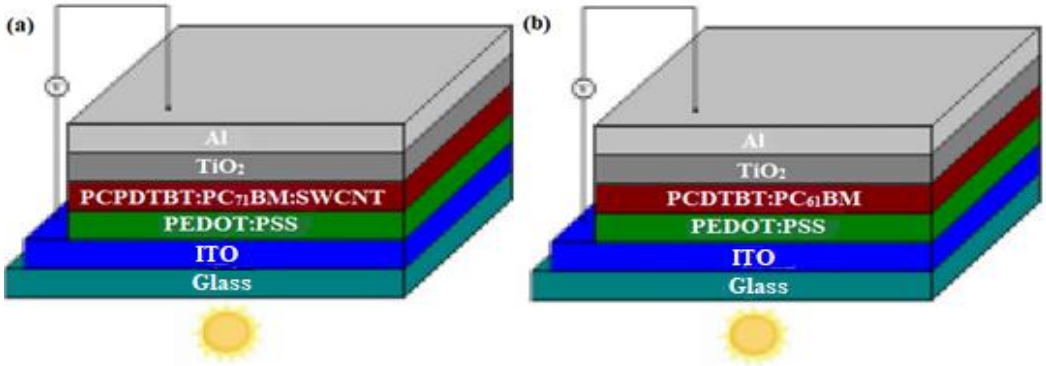

Fig. 1. Devices diagrams for the (A) PCPDTBT:$PC_{71}BM$:SWCNTs and (B) PCPDTBT:$PC_{61}BM$-based devices being investigated

factor (FF) and its total light-to-electrical energy conversion efficiency (PCE).

$$\mathrm{PCE}\ (\%) = \frac{J_{max}V_{max}}{P_{in}} \quad (1)$$

$$\mathrm{FF} = \frac{J_{max}V_{max}}{J_{sc}\ V_{oc}} \quad (2)$$

In these equations, J_{sc} signifies the short circuit density (mA/cm^2), V_{oc} is indicative of the open-circuit voltage (V), J_{max} (mA/cm^2) and V_{max} (V) indicate the current density and voltage when there is highest power output in the J-V curves, respectively, and P_{in} refers to the incident light power. Moreover, DropSens interdigitated Platinum electrodes (IDEs) were used to find out the electrical conductivity. Using the following equation, these IDEs can help determine the surface conductivity (σ) of the samples [1].

$$\sigma = \frac{i}{V}\frac{n}{\mathcal{W}t\ell} \quad (3)$$

Here, refers to the film thickness, refers to how far the fingers are from each other (6.67mm), indicates the number of fingers (500), and signifies how far the electrodes are from each other (5µm).

RESULTS AND DISCUSSION

Effect of Treatment on PEDO: PSS Properties

The transmittance spectra of the PEDOT:PSS-based layer prior to and following the treatment are demonstrated in Fig. 2.

The transmittance intensity increases to some extent after the PEDOT:PSS layer has undergone treatment. The highest transmittance of around 91% has been exhibited by the pure PEDOT:PSS layer, which is around 450 nm. It can be seen in Fig. 2 that when the PEDOT:PSS is doped with EG and DMSO, there is a small increase in the transmittance spectra. It is determined that the increased transparency is advantageous for the OSCs electronics [24]. Following solvent treatment, it is seen that the transparency of the PEDOT:PSS increases further. Good transmittance spectra are typically exhibited by all the PEDOT:PSS thin films, ranging between 400 and 800 nm, which may be because of the colourless attribute of the PSS. The presence of PEDOT is what essentially gives rise to optical absorption in PEDOT:PSS [25]. The loss of PSS from the PEDOT:PSS thin films are not the reason for this variation in intensity since heating was used to eliminate all solvents from the PEDOT:PSS films and no solvent was used to rinse the treated PEDOT:PSS films. Hence, the variation in transmittance may be because of a solvent-induced change in the morphology of the PEDOT:PSS films. A simple model was presented by [12] that used the Beer-Lambert law to determine the variations in intensities following the treatment of PEDOT:PSS layer with solvents.

According to the authors, there are distinct transmittance intensities of the PEDOT:PSS

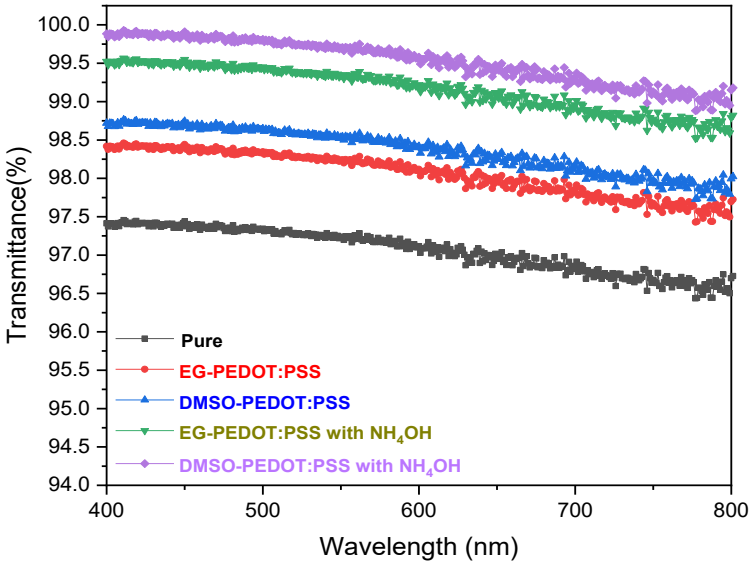

Fig. 2. Optical transmittance of PEDO:PSS electrodes, pure and DMSO and EG-treated.

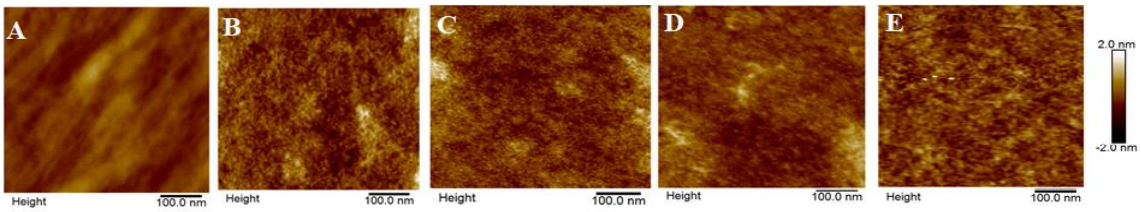

Fig. 3. AFM images of (A) a pristine PEDOT:PSS film and doped by (B) EG, and (C) DMSO; (D) EG-PEDOT:PSS with NH_4OH and (E) DMSO- PEDOT:PSS with NH_4OH

layers, depending on the extent to which the substrate uniformly covers the PEDOT:PSS. The authors noted that there is an increase in the transmittance properties of PEDOT:PSS following solvent treatment, implying the accumulation of the PSS chains [12].

This study obtained similar findings, with the AFM images confirming the PSS aggregation Fig. 3. According to AFM images, the solvent additives affect the surface morphology of the PEDOT:PSS. It is determined that the pure PEDOT:PSS layer has a surface roughness of 0.98nm. Following doping with EG, this increased to 1.03 nm. The surface roughness increased to 1.18 nm following the doping of PEDOT:PSS with DMSO, which confirms the aggregation of PSS. It is observed that with further treatment, there is additional PSS separation and an increase in rough surface. A rougher surface of 2.1 nm is noted for NH4OH solvent treated EG doped PEDOT:PSS layer, while for NH4OH solvent treated DMSO doped PEDOT:PSS layer, the surface roughness was found to be 2 nm. it is possible for the contact area between the PEDOT:PSS and the active layer to increase with the increase in surface roughness, which enhances hole extraction to the anode [1]. PEDOT and PSS sites also experience phase separation following treatment, and this also plays a part in increasing the PEDOT:PSS layers' electrical conductivity.. There is also an increase in electrical conductivity

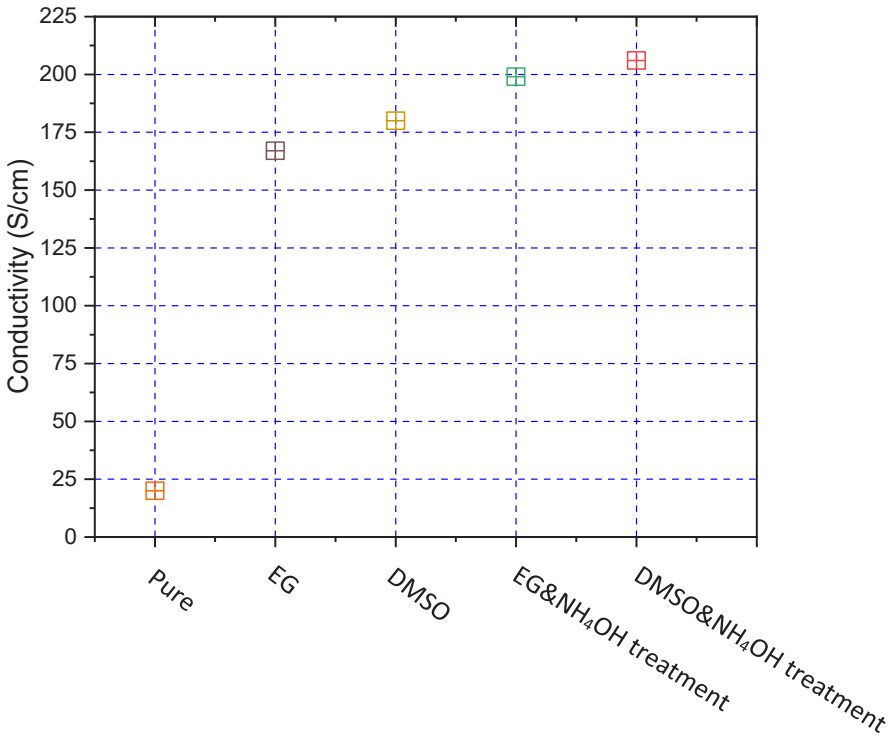

Fig. 4. Variation of the conductivity of the PEDOT:PSS film treated without and with.

following the doping of PEDOT:PSS with EG from 20±3S/cm to167±4S/cm, as can be seen in Fig. 4. When the EG doped PEDOT:PSS layer is made to undergo NH4OH solvent treatment for some hours, there is a further increase in conductivity, which leads to PEDOT and PSS experiencing a greater degree of site separation, and the electrical conductivity increases substantially to 199±7S/cm. When DMSO is used as doping material (180±8S/cm) and when solvent treatment (206±6S/cm) is carried out, similar outcomes are obtained. It is believed that the conductivity increases in the presence of solvent because of the changes in the PEDOT:PSS morphology, which gives rise to improved links between conducting PEDOT chains.

It has been suggested that the chemical composition of the solvents is responsible to a large extent for the increase in conductivity. There is an increase in electrical conductivity when DMSO solvents are used, which was considered to occur because of the phase separation of additional PSS. Thus, a decrease in insulation is experienced by the conducting PEDOT:PSS domains [26]. The PEDOT:PSS has greater conductivity, because of which there may be a decrease in the interface contact barrier, with the photo-induced carrier transporting experiencing an increase, which leads to an increase in the short circuit current density [27]. The PEDOT:PSS thin films undergo deformation following treatment, which is examined using Raman spectroscopy, the results of which are presented in Fig. 5 (A and B). It has been observed that the Raman spectra of the pure and the additive-treated PEDOT:PSS films is between 1400 and 1600 cm^{-1}. PEDOT vibrational models (C-C) are situated at 1449cm^{-1}, and following doping with EG, DMSO, EG with NH4OH solvent treatment and DMSO with NH4OH solvent treatment, this changes to 1450cm^{-1}, 1448cm^{-1}, 1447cm^{-1} and 1445cm^{-1}, respectively. It is also observed that there is an additional vibrational mode of PEDOT:PSS attributed to C-C stretching at approximately 1400cm^{-1} as well as 1525cm^{-1}, whereas the vibrational mode of PSS is situated at approximately 1560 cm^{-1} [28]. It is suggested by the Raman shift in the PEDOT vibrational mode that following the treatment, PEDOT switches to linear structure from coil shape [29].

With the Raman fingerprints' intensity has decreased, there is a partial removal of PSS [30]. When there is a linear orientation of the polymer chains when the neighbouring thiophene rings are mainly arranged in the same plane, there should be a delocalization of the conjugated π-electrons across the entire polymer chain, which would lead to greater charge-carrier mobility in comparison to the coil structure [29]. Hence, there is an increase in the strength of the interaction between PEDOT chains, and there can be improvements in inter-chain and interchain charge-carrier mobility; thus,

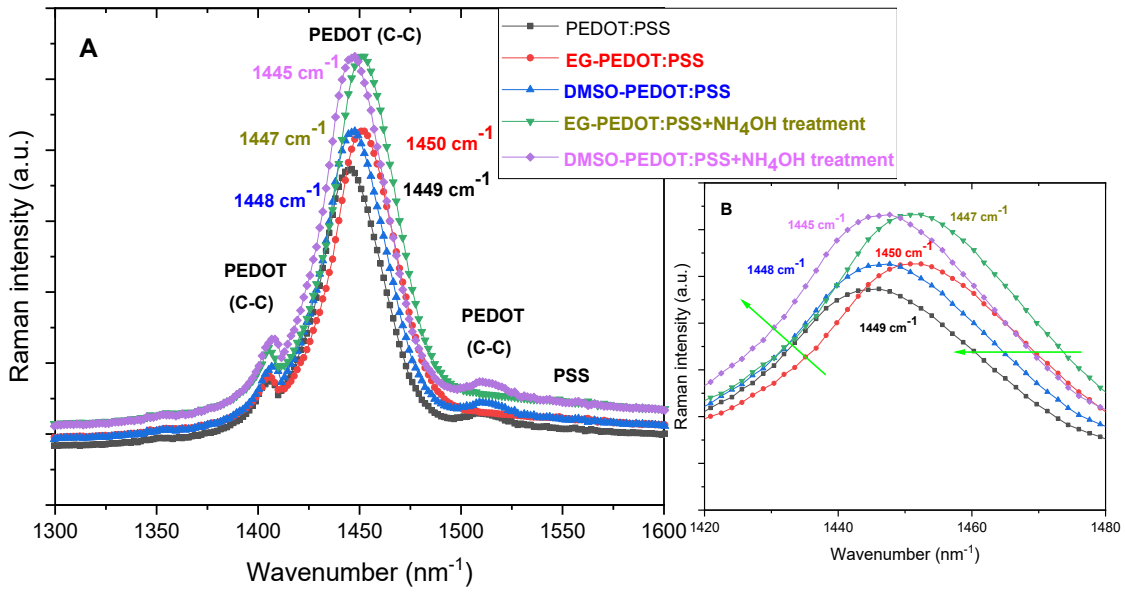

Fig. 5. (A) Raman spectra of the (PEDOT:PSS) film treated without and with, and (B) the highest peak is about 1450cm^{-1}

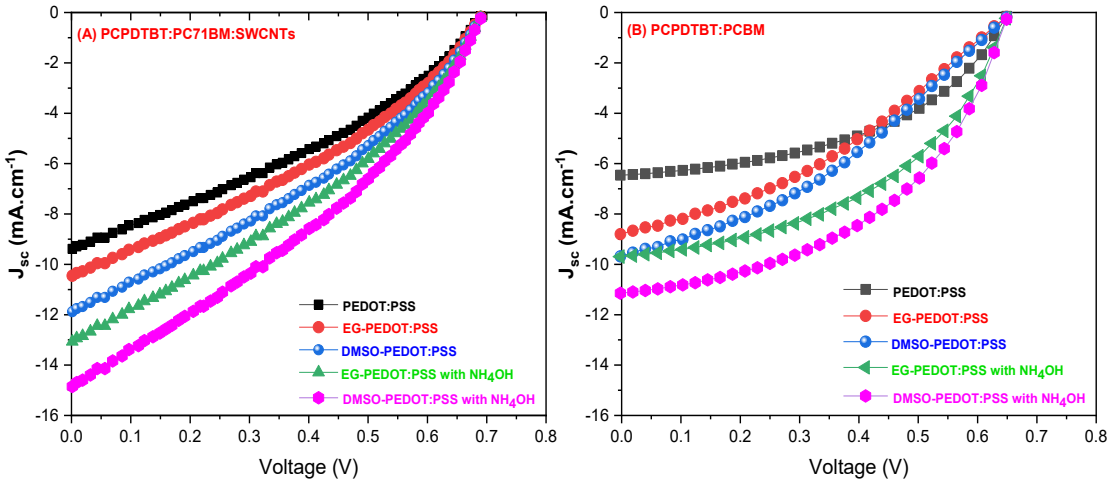

Fig. 6. Shows the J-V characteristics of solar cells made of (A) PCPDTBT: $PC_{71}BM$:SWCNTs and (B) PCPDTBT: $PC_{61}BM$.

there is an increase in conductivity as explained before.

Solar Cell Characteristics

Two distinct mixtures with two distinct conjugated polymers, PCPDTBT: $PC_{71}BM$:SWCNTs and PCPDTBT:$PC_{61}BM$ are used to study the impact of treated and untreated PEDOT:PSS on the photovoltaic characteristics as demonstrated in Fig. 6 (A and B). After the PEDOT:PSS layer is doped with EG and DMSO and following the solvent treatment, the short circuit current density (J_{SC}) undergoes a significant increase as depicted in Tables 1 and 2.

Fig. 6A shows how this treatment influences PCPDTBT: $PC_{71}BM$:SWCNTs-based solar cells.

There is an increase in J_{SC} from 9.28mA/cm^2 in the device utilizing a pure PEDOT:PSS layer to 10.45mA/cm^2 and 11.08mA/cm^2 for PEDOT:PSS layers doped with EG and DMSO, respectively. Identical behaviour is noted for PCPDTBT:$PC_{61}BM$-based solar cells, where J_{SC} in the device that uses a pure PEDOT:PSS layer is 6.4mA/cm^2, which increases to 8.66mA/cm^2 and 9.4mA/cm^2 in PEDOT:PSS layers doped with EG and DMSO, respectively. When the treated PEDOT:PSS layers undergo a solvent treatment, there is an additional increase in J_{SC} as shown in Tables 1 and 2. It is believed that the short circuit current density increases following their doping, the electrical conductivity of the PEDOT:PSS layers rises, which decreases the interface contact barrier and thus enhances the photo-induced carrier transporting [27]. In addition, because the surface roughness increases, there may be an increase in the contact area between the PEDOT:PSS and the active layer, which enhances the hole extraction to the anode [1]. Following treatment, the coarse surface of the PEDOT:PSS layer can possibly cause the light scattering that enters the active layer to increase [31], and the light propagation path in the active layer may thus become lengthier [23].

It has been confirmed that there is an increase in Jsc in the device which is being examined for determining the incident photon-to-current collection efficiency (IPCE) spectra of PCPDTBT:$PC_{71}BM$:SWCNTs as well as PCPDTBT: $PC_{61}BM$-based devices utilizing PEDOT:PSS based,

Table 1. Photovoltaic parameters cells of PCPDTBT:PC71BM:SWCNTs-based solar

PCDTBT:$PC_{71}BM$:SWCNTs	Pure	EG	DMSO	With solvent treatment	
					NH_4OH
J_{SC} (mA/cm^2)	9.28	10.45	11.8	12.93	14.84
V_{OC} (V)	0.68	0.68	0.68	0.68	0.69
FF	0.35	0.34	0.34	0.35	0.36
PCE %	2.20	2.41	2.72	3.07	3.68
R_S (Ω)	98	94	92	86	87

Table 2. Photovoltaic parameters cells of PCDTBT:PC61BM-based solar

PCDTBT:$PC_{61}BM$	Pure	EG	DMSO	With solvent treatment	
					NH_4OH
J_{SC} (mA/cm²)	6.4	8.66	9.4	9.65	11.09
V_{OC} (V)	0.64	0.64	0.64	0.64	0.64
FF	0.37	0.35	0.35	0.38	0.39
PCE %	1.51	1.93	2.1	2.34	2.76
R_S (Ω)	67	62	61	60	58

and without treatment as a buffer layer can be seen in Fig. 7. The familiar spectral response of its bulk heterojunction mixture is demonstrated by every device. The highest (IPCE) is shown by the PCPDTBT:PC_{71}BM:SWCNTs-based devices of around 40% at wavelengths of approximately 630-680 nm [32]. There are two major peaks of the PCPDTBT:PC_{61}BM-based device, the first is around 30% at wavelengths of approximately 600-650 nm [33]. In addition, for all the devices examined, no change is noted in the open circuit voltage (V_{OC}). The equation given below is fundamentally used to determine V_{OC}:

$$V_{OC} = [\text{LUMO}_{\text{acceptor}} - \text{HOMO}_{\text{donor}}] - 0.3 \quad (4)$$

For the PCPDTBT:PC_{71}BM:SWCNTs based devices, a higher V_{OC} is obtained between 0.69±0.02V and 0.64±0.02V for devices based on PCPDTBT:PC_{61}BM as can be seen in Tables 1 and 2. FF values are also found to vary for PCPDTBT:PC_{71}BM:SWCNTs based devices, increasing from 0.35 in devices based on pure PEDOT:PSS (PCPDTBT:PC_{71}BM:SWCNTs mixture) to 0.36 in the device using PEDOT:PSS doped with DMSO and NH4OH solvent treatment (for PCPDTBT:PC_{71}BM:SWCNTs mixture). PCPDTBT:PC_{61}BM based devices; however, they have an FF value are increasing from 0.37 to 0.39. This increase may be because after the PEDOT:PSS layer is doped, there may be an increase in the series resistance (refer to Tables 1 and 2). It was explained previously that this increase has a correlation with the increase in the PEDOT:PSS layer's electrical conductivity. PCPDTBT:PCBM based devices generally exhibit low FF because of the low crystallinity exhibited by the PCPDTBT material that has a bulk side chain [34]. For the devices studied, the power conversion efficiency (PCE) is shown in Table 1 and Table 2. PCE of 2.20% is noted for the pure PEDOT:PSS for PCPDTBT:PC_{71}BM:SWCNTs based device. For the device using PEDOT:PSS doped with DMSO and NH4OH solvent treatment, the PCE increases to 3.68%, which is essential because the short circuit current density increases [34].

Similar behaviour is noted for the

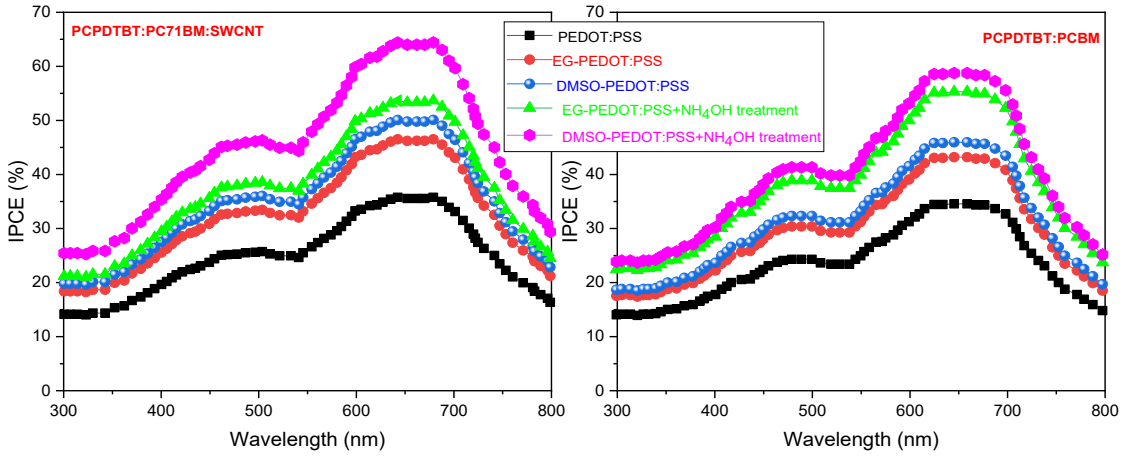

Fig. 7. IPCE spectra for devices based on PCPDTBT:PC71BM:SWCNTs and PCPDTBT:PC61BM.

PCPDTBT:PC_{61}BM based devices, where a PCE of 1.51% was obtained for the device with untreated PEDOT:PSS. The PCE increased to 2.76% in the device using PEDOT:PSS doped with DMSO and NH4OH solvent treatment. The reason this rise is experienced is because the short circuit current density increases [24,34], and also because of the evident increase in FF.

CONCLUSION

To sum up, there is a direct effect of improving PEDOT:PSS properties on the performance of the organic solar cells (OSCs) which are being examined. There were two ways in which the PEDOT:PSS treatments were performed. The first was doping it with DMSO and EG while the second involved the solvent treatment using the NH4OH solvent. The use of PCPDTBT:PC_{71}BM:SWCNTs blend as an active layer in the organic solar cells depicts a minor enhancement in the performance of devices in comparison to those in which the active layer is PCPDTBT:PC_{61}BM. It has been determined in this study that a vital part is performed by the conductivity of PEDOT:PSS in improving the organic devices.

CONFLICT OF INTEREST

The authors declare that there is no conflict of interests regarding the publication of this manuscript.

REFERENCES

1. Saghaei J, Fallahzadeh A, Saghaei T. ITO-free organic solar cells using highly conductive phenol-treated PEDOT:PSS anodes. Org Electron. 2015;24:188-194.
2. Guguloth L, Singh K, Reddy Channu VS, Kumari K. Improved performance of ternary blend polymer solar cells via work function tuning and suppressed interface recombination using hybrid PEDOT:PSS-graphene oxide hole transport layer. Appl Surf Sci. 2021;540:148266.
3. Khasim S, Pasha A, Lakshmi M, Chellasamy P, Kadarkarai M, Darwish AAA, et al. Post treated PEDOT-PSS films with excellent conductivity and optical properties as multifunctional flexible electrodes for possible optoelectronic and energy storage applications. Opt Mater. 2022;125:112109.
4. Zhang S, Fan Z, Wang X, Zhang Z, Ouyang J. Enhancement of the thermoelectric properties of PEDOT:PSS one-step treatment with cosolvents or their solutions of organic salts. Journal of Materials Chemistry A. 2018;6(16):7080-7087.
5. Wu Z, Yu Z, Yu H, Huang X, Chen M. Effect of trifluoroacetic acid treatment of PEDOT:PSS layers on the performance and stability of organic solar cells. Journal of Materials Science: Materials in Electronics. 2018;29(8):6607-6618.
6. Mahato S, Puigdollers J, Voz C, Mukhopadhyay M, Mukherjee M, Hazra S. Near 5% DMSO is the best: A structural investigation of PEDOT: PSS thin films with strong emphasis on surface and interface for hybrid solar cell. Appl Surf Sci. 2020;499:143967.
7. Yu R, Wu G, Tan Za. Realization of high performance for PM6:Y6 based organic photovoltaic cells. Journal of Energy Chemistry. 2021;61:29-46.
8. Xu Y, Jia Y, Liu P, Jiang Q, Hu D, Ma Y. Poly(3,4-ethylenedioxythiophene) (PEDOT) as promising thermoelectric materials and devices. Chem Eng J. 2021;404:126552.
9. Masoumi S, O'Shaughnessy S, Pakdel A. Organic-based flexible thermoelectric generators: From materials to devices. Nano Energy. 2022;92:106774.
10. Smida N, Zaidi B, Althobaiti MG. Anthracene / fluorescein based semi-conducting polymer for organic photovoltaics: Synthesis, DFT, optical and electrical properties. J Mol Struct. 2023;1272:134088.
11. Dianetti M, Di Giacomo F, Polino G, Ciceroni C, Liscio A, D'Epifanio A, et al. TCO-free flexible organo metal trihalide perovskite planar-heterojunction solar cells. Sol Energy Mater Sol Cells. 2015;140:150-157.
12. Wang W, Qin F, Jiang X, Zhu X, Hu L, Xie C, et al. Patterning of PEDOT-PSS via nanosecond laser ablation and acid treatment for organic solar cells. Org Electron. 2020;87:105954.
13. Ramadhan ZR, Han JW, Hong J, Park SB, Kim JH, Wibowo AF, et al. Conductive PEDOT:PSS on surface-functionalized chitosan biopolymers for stretchable skin-like electronics. Org Electron. 2021;94:106165.
14. Liu Z, Parvez K, Li R, Dong R, Feng X, Müllen K. Transparent Conductive Electrodes from Graphene/PEDOT:PSS Hybrid Inks for Ultrathin Organic Photodetectors. Adv Mater. 2014;27(4):669-675.
15. Alkhalayfeh MA, Aziz AA, Pakhuruddin MZ. Enhancing the efficiency of polymer solar cells by embedding Au@Ag NPs Durian shape in buffer layer. Solar Energy. 2021;214:565-574.
16. Mkawi EM, Al-Hadeethi Y, Bazuhair RS, yousef As, Shalaan E, Arkook B, et al. Fabricated Cu_2Zn SnS_4 (CZTS) nanoparticles as an additive in P3HT: PCBM active layer for efficiency improvement of polymer solar cell. J Lumin. 2021;240:118420.
17. Liu G, Zheng L, Sun Y, Zhang M, Xiong C. Preparation of flexible conductive composite electrode film of PEDOT:PSS/Aramid nanofibers via vacuum-assisted filtration and acid post-treatment for efficient solid-state supercapacitor. Int J Hydrogen Energy. 2022;47(53):22454-22468.
18. Ino T, Hayashi T, Ueno K, Shirai H. Atmospheric-pressure argon plasma etching of spin-coated 3,4-polyethylenedioxythiophene:polystyrenesulfonic acid (PEDOT:PSS) films for cupper phtalocyanine (CuPc)/C60 heterojunction thin-film solar cells. Thin Solid Films. 2011;519(20):6834-6839.
19. Guo Q, Lin J, Dong X, Zhu L, Guo X, Liu F, et al. Optimized molecular aggregation via incorporating fluorinated unit in the polymer donor for 17.3% efficiency organic solar cells. Chem Eng J. 2022;431:134117.
20. Fernández-Arteaga Y, Maldonado J-L, Nicasio-Collazo J, Meneses-Nava M-A, Rodríguez M, Barbosa-García O, et al. Solution processable graphene derivative used in a bilayer anode with conductive PEDOT:PSS on the non-fullerene PBDB-T:ITIC based organic solar cells. Solar Energy. 2021;225:656-665.
21. Markose KK, Jasna M, Subha PP, Antony A, Jayaraj MK.

Performance enhancement of organic/Si solar cell using CNT embedded hole selective layer. Solar Energy. 2020;211:158-166.
22. Lee J-H, Shin H-S, Na S-I, Kim H-K. Transparent and flexible PEDOT:PSS electrodes passivated by thin IZTO film using plasma-damage free linear facing target sputtering for flexible organic solar cells. Sol Energy Mater Sol Cells. 2013;109:192-198.
23. Kadem BY, Al-hashimi MK, Hassan AK. The Effect of Solution Processing on the Power Conversion Efficiency of P3HT-based Organic Solar Cells. Energy Procedia. 2014;50:237-245.
24. Hegde R, Henry N, Whittle B, Zang H, Hu B, Chen J, et al. The impact of controlled solvent exposure on the morphology, structure and function of bulk heterojunction solar cells. Sol Energy Mater Sol Cells. 2012;107:112-124.
25. Huang L-M, Peng C-Y, Hu C-W, Lu H-C, Chen C-H, Yang D-J, et al. Spectroelectrochemical and adhesion properties of chemically synthesized ion conducting poly (vinyl butyral) in Prussian blue and poly (3, 4-ethylenedioxythiophene) laminated electrochromic glazing. Sol Energy Mater Sol Cells. 2017;171:258-266.
26. Raj A, Kumar M, Anshul A. Recent advancement in inorganic-organic electron transport layers in perovskite solar cell: current status and future outlook. Materials Today Chemistry. 2021;22:100595.
27. Farah AA, Rutledge SA, Schaarschmidt A, Lai R, Freedman JP, Helmy AS. Conductivity enhancement of poly(3,4-ethylenedioxythiophene)-poly(styrenesulfonate) films post-spincasting. J Appl Phys. 2012;112(11):113709.
28. Chaturvedi N, Swami SK, Dutta V. Spray deposition of poly(3-hexylthiophene) and [6,6]-phenyl-C61-butyric acid methyl ester blend under electric field for improved interface and organic solar cell characteristics. Thin Solid Films. 2016;598:82-87.
29. Sheng Hsiung C, Chien-Hung C, Feng-Sheng K, Chuen-Lin T, Chun-Guey W. Unraveling the Enhanced Electrical Conductivity of PEDOT:PSS Thin Films for ITO-Free Organic Photovoltaics. IEEE Photonics Journal. 2014;6(4):1-7.
30. Kadem BY, Kadhim RG, Banimuslem H. Efficient P3HT:SWCNTs hybrids as hole transport layer in P3HT:PCBM organic solar cells. Journal of Materials Science: Materials in Electronics. 2018;29(11):9418-9426.
31. Rasool S, Hoang QV, Vu DV, Song CE, Lee HK, Lee SK, et al. High-efficiency single and tandem fullerene solar cells with asymmetric monofluorinated diketopyrrolopyrrole-based polymer. Journal of Energy Chemistry. 2022;64:236-245.
32. Liu Z, Wang N. Ternary organic solar cells with NC70BA as a third component material exhibit high open-circuit voltage and small energy losses. J Power Sources. 2020;448:227442.
33. Hwang H, Lee H, Shafian S, Lee W, Seok J, Ryu K, et al. Thermally Stable Bulk Heterojunction Prepared by Sequential Deposition of Nanostructured Polymer and Fullerene. Polymers. 2017;9(12):456.
34. Barulina E, Khodr A, Dkhil SB, Perkhun P, Quiroz YAA, Koganezawa T, et al. Improved ultraviolet stability of fullerene-based organic solar cells through light-induced enlargement and crystallization of fullerene domains. Thin Solid Films. 2022;757:139394.